

Modelling the Corrosion Related EM Signatures of Ships.

P. Allan and A. Watt
Department of Physics and Astronomy
The University of Glasgow
Scotland

February 26, 2004

Abstract

The electromagnetic fields from corrosion currents and corrosion protection devices contribute to the underwater EM signatures of marine vessels. These fields are of interest as they affect the susceptibility of the vessel to underwater multi-influence mines and provide insight into the protection offered against corrosion. Therefore there have been many approaches developed to evaluate these corrosion related signatures.

The method presented here involves using a boundary element method (BEM). The surface of the domain is meshed using triangular elements, and the BEM equations are formed using normalised moments for these elements. This allows the required integrals to be calculated by polynomials. These equations are solved using a point successive over-relaxation method (PSOM) providing values for the potential and its normal derivative on the boundary. The magnetic fields are evaluated using a new approach which eliminates the requirement to mesh the volume of the domain.

Calculations were performed for a model hull in a box of seawater. The model consisted of 5132 surface elements. Each iteration of the PSOM took about one second on a normal PC. The speed of convergence depended on the integrity of the paintwork on the hull. For high resistance films, the method was extremely stable and a few hundred iterations were sufficient, while several thousand were needed for low resistance films with the currents emanating from ICCP anodes. Calculations to date have explored the algorithm and convergence, without too much emphasis on polarization data or comparison with experimental data, which is subject to further development.

1 Introduction

The electromagnetic signatures of marine vessels due to corrosion and corrosion protection devices are important for detection and identification purposes (Jeffery & Brooking [1]). Corrosion currents in the sea around the vessel give rise to characteristic electric and magnetic

fields. This paper considers how information on the electrochemical potentials at the interface between the hull and seawater may be used to calculate an electric potential around the vessel. As seawater is conducting, currents flow in the water and magnetic fields result. We confine ourselves to considering static fields although both static and low frequency fields are present. This problem has already been studied in the literature (Zamani & Porter [2], Wang *et al.* [3]) but we believe that alternative methods may be used which have some advantages.

We assume the sea is represented by a finite rectangular box with insulating boundaries which is filled with homogeneous seawater and the ship is floating centrally on the top surface. The task of calculating the electromagnetic fields in the box may be addressed by various methods, but we choose the Boundary Element Method (BEM) as the water is homogeneous. The "boundary" in this case is the bottom of the box, its front, rear, left and right faces, the surface of the submerged part of the hull and propeller, and that part of the surface of the sea on the top face outside the vessel. The boundary is then covered with discrete elements which we choose to be triangles. The nodes in the problem are taken to be the centroids of the triangles, and the electric potential over a triangle is assumed to be the same as its value at its centroid (i.e. constant elements).

2 Implementation of the BEM.

The derivation of the BEM form considered in this work can be found in Brebbia [4]. The basic equation describing the model is

$$H\mathbf{u} = G\mathbf{q} \quad (2.1)$$

where, for this model of a ship corroding in seawater, \mathbf{u} is a vector of the potentials on each element, and \mathbf{q} is the outward normal derivative of the potential on each element. This may also be thought of as the negative of the outward normal component of electric field emitted from each element.

The governing equation within the domain can be shown (Brebbia [4]) to be Laplace's Equation, which in three dimensions has solution

$$\frac{1}{4\pi R_{i,j}}. \quad (2.2)$$

This function is used as the weighting function in the calculation of the coefficient matrices in eqn (2.1), where matrices elements are obtained as follows

$$H_{i,j} = \begin{cases} \frac{1}{4\pi} \int_{\Gamma_j} \frac{\partial}{\partial \mathbf{n}} \left(\frac{1}{R_{i,j}} \right) d\Gamma, & \text{when } i \neq j, \\ \frac{1}{4\pi} \int_{\Gamma_j} \frac{\partial}{\partial \mathbf{n}} \left(\frac{1}{R_{i,j}} \right) d\Gamma + \frac{1}{2}, & \text{when } i = j \end{cases} \quad (2.3)$$

$$G_{i,j} = \frac{1}{4\pi} \int_{\Gamma_j} \frac{1}{R_{i,j}} d\Gamma_j, \quad \forall i, j \quad (2.4)$$

where Γ_j is the surface of triangle j and \mathbf{n} is the outward unit normal to Γ_j .

Here the ‘ i ’ subscript indicates the source element whilst ‘ j ’ refers to the element over which the integral is evaluated.

The method used to compute the necessary integrals is taken from Allan [12], and Allan & Watt [13]. This method involved the adoption of a local coordinate system for each element integrated over which placed the element on a (x, y) plane with origin at the element’s centroid. By removing all the scaling from the triangular elements, it is possible to calculate normalised moments for the triangle which depend only on a unique shape parameter of the triangle.

With these known, the required integration can be calculated by forming a polynomial with the unique shape parameter as the variable, and then differentiating. This method has been tested against more conventional ones and has been shown to provide extremely accurate values (Allan & Watt [13]).

Once formed, eqn (2.1) was solved using a point successive over-relaxation method (PSOM) (Jansson [8]). This scheme has a major advantage over more popular ones used for solving large sets of equations in that it allows direct manipulation of boundary conditions for each individual unknown as it iteratively seeks solutions. On the outer surfaces of the seawater box, the boundary conditions are relatively simple. If you wish the box to be insulating, the \mathbf{q} values can be set to zero, whilst if you wish them to be conducting, the \mathbf{u} values may be set to zero. On the hull and propeller, complex polarization relations linking u and q for each element need to be applied (Adey *et al.* [10], Zamani & Porter [2]), although for the analysis reported here, a linear relation has been used.

Starting values of the quantities \mathbf{u} and \mathbf{q} are guessed and then the discrepancy between the i^{th} elements of $H\mathbf{u}$ and $G\mathbf{q}$ is regarded as an indicator of the defects in the values of u_i and q_i : one may write

$$\tilde{u}_i = u_i + \frac{r}{H_{ii}} ((H\mathbf{u})_i - (G\mathbf{q})_i) \quad (2.5)$$

where the old values of \mathbf{u} and \mathbf{q} are used on the right to compute a new value of \tilde{u}_i on the left. Here r is a relaxation factor which may be greater than 1 (over-relaxation) or much less than 1 if a more delicate touch is needed to obtain convergence. As soon as a new value of u_i is calculated, the corresponding q_i can be calculated from the polarization relation on element i . The procedure is repeated for all i , then iterated until convergence is obtained. It is straightforward to incorporate other conditions onto the elements, i.e. an Impressed Current Cathodic Protection (ICCP) system can easily be modelled where there are anodes attached to the hull which fix the values for u and q at the relevant elements (Zamani & Porter [2]).

3 Calculation of the Electromagnetic Fields

Once the equations have been solved as outlined above, values for u and q are known for every element on the boundary of the model. All that remains is to calculate the electromagnetic fields due to these potentials and their derivatives at positions within the domain.

3.1 Electric Fields

While deriving the theory behind the BEM (Brebbia [4]) an equation appears which provides the potential at a point (i, j, k) within the domain,

$$V_{ijk} = \sum_{p=1}^n q_p G_{ijk,p} - \sum_{p=1}^n u_p H_{ijk,p}. \quad (3.1)$$

The matrices G and H will need to be recalculated for eqn (3.1) to be used since the point (i, j, k) is not one for which the matrix elements have been previously calculated. Once the potentials have been calculated, the application of numerical differentiation to calculate the negative of the gradient of V at this point provides the electric field. Obviously the number of points at which the potential must be calculated depends on the algorithm used for the numerical differentiation but despite this it is a fairly direct process to calculate the electric field. Alternatively, the electric field may be calculated directly from the \mathbf{u} and \mathbf{q} vectors (Allan [12]).

3.2 Magnetic Fields

The method usually adopted by industry appears to be the following. The interior of the domain is meshed and \mathbf{E} is calculated at each node (Kermorgant [11]). From this the current density can be calculated and then the magnetic field at a point can be calculated by the Biot-Savarts Law which becomes the following summation over the entire volume

$$\mathbf{H} = \frac{1}{4\pi} \sum_V \frac{\mathbf{J} \times \mathbf{R}}{R^3} dV. \quad (3.2)$$

The main drawback of this method is that after having used BEM to restrict the mesh to the boundary to calculate u and q , it is undesirable to now mesh the entire volume of the domain. However, all the relations used to arrive at the magnetic field strength are linear which implies that a linear formula exists which goes straight from the \mathbf{u} and \mathbf{q} values to \mathbf{H} .

A numerical calculation of the magnetic field from surface potentials using a simple test geometry of a cube showed that it is indeed plausible to calculate the magnetic field at an arbitrary point within the domain directly from the surface potentials. Before embarking on a proof of this, it is necessary to state explicitly what is being claimed. We are claiming that the magnetic field arising from the current within an arbitrary conducting domain with no internal sources of current can be calculated solely from the electric potential on the boundary.

3.2.1 Vector Identities and Theorems

The following vector identities and theorem can be found in most textbooks that cover vector calculus (Lorrain *et al.* [16]). Nonetheless, since they play a crucial role in the development of a proof of the conjectured theorem, they have been quoted below along with a proof for the theorem.

Identity 1. Let f be a scalar function and \mathbf{A} a vector function, then

$$\nabla \cdot (f\mathbf{A}) = (\nabla f) \cdot \mathbf{A} + f (\nabla \cdot \mathbf{A}).$$

Identity 2. Let a and b be scalar functions, then

$$\nabla (ab) = a\nabla b + b\nabla a.$$

Identity 3. Let f be a scalar function, then

$$\nabla \times (\nabla f) = 0.$$

Identity 4. Let f be a scalar function and \mathbf{A} a vector function, then

$$\nabla \times (f\mathbf{A}) = (\nabla f) \times \mathbf{A} + f (\nabla \times \mathbf{A}).$$

Identity 5. Let \mathbf{A} be a vector function and let v be a volume enclosed by the surface s , with ds pointing in the direction of the unit normal out of the volume, then

$$\int_s \mathbf{A} \times ds = - \int_v (\nabla \times \mathbf{A}) dv$$

Identity 6. Consider a vector \mathbf{R} such that $\mathbf{R} = \mathbf{r} - \mathbf{r}'$ (where $\mathbf{r} = (x, y, z)$ and $\mathbf{r}' = (x', y', z')$). Then

$$\nabla' \frac{1}{R} = -\nabla \frac{1}{R}.$$

Theorem 1. For any function f ,

$$\int_v \nabla f dv = \int_s f ds \tag{3.3}$$

where v is a volume bounded by the surface s , and ds points in the direction of the unit normal out of the volume.

Proof. Let \mathbf{a} be any constant vector. Using vector identity 1

$$\begin{aligned} \mathbf{a} \cdot \int_v \nabla f dv &= \int_v \nabla \cdot (f\mathbf{a}) dv - \int_v f (\nabla \cdot \mathbf{a}) dv \\ &= \int_s f\mathbf{a} \cdot ds - 0 \text{ (from the divergence theorem and } \nabla \cdot \mathbf{a} = 0) \\ &= \mathbf{a} \cdot \int_s f ds. \end{aligned}$$

Since \mathbf{a} is an arbitrary vector,

$$\int_v \nabla f dv = \int_s f ds.$$

□

3.2.2 Proof of the Theorem

We begin the proof of this statement by considering the following example. There exists a current source with density \mathbf{J}' in a volume dv' at position \mathbf{r}' , so the Boit-Savarts Law states that the magnetic flux density at an arbitrary point \mathbf{r} may be written as

$$d\mathbf{B} = \frac{\mu_0}{4\pi} \frac{\mathbf{J}' \times \mathbf{R}}{R^3} dv' \quad (\text{where } \mathbf{R} = \mathbf{r} - \mathbf{r}'). \quad (3.4)$$

This can be expressed using the vector potential as

$$d\mathbf{B} = \nabla \times d\mathbf{A} \quad \text{with} \quad d\mathbf{A} = \left(\frac{\mu_0}{4\pi} \frac{\mathbf{J}'}{R} \right) dv'. \quad (3.5)$$

To find \mathbf{A} it is necessary to integrate over the entire volume v' , but we may also note that $\mathbf{J}' = \sigma' \mathbf{E}' = -\sigma' \nabla' u'$ where σ' is the conductivity at the point \mathbf{r}' and u' is the electric potential there. Therefore the necessary integral may be expressed as

$$\mathbf{A} = -\frac{\mu_0}{4\pi} \int_{v'} \left(\frac{\sigma'}{R} \nabla' u' \right) dv' \quad (3.6)$$

Using theorem 1 found in subsection 3.2.1, along with some basic vector identities quoted there, transforms eqn (3.6) into

$$\mathbf{A} = -\frac{\mu_0}{4\pi} \int_{s'} \frac{\sigma' u'}{R} ds' + \frac{\mu_0}{4\pi} \int_{v'} u' \left\{ \frac{1}{R} \nabla' \sigma' + \sigma' \nabla' \left(\frac{1}{R} \right) \right\} dv'. \quad (3.7)$$

Identity 6 allows the final term in the above to be written as

$$\frac{\mu_0}{4\pi} \int_{v'} \sigma' u' \nabla' \left(\frac{1}{R} \right) dv' = -\nabla \left(\frac{\mu_0}{4\pi} \int_{v'} \sigma' u' \left(\frac{1}{R} \right) dv' \right).$$

The necessary application of curl to this gradient terms results in it making no contribution to the magnetic field which leaves

$$\mathbf{A} = -\frac{\mu_0}{4\pi} \int_{s'} \frac{\sigma' u'}{R} ds' + \frac{\mu_0}{4\pi} \int_{v'} \frac{u'}{R} (\nabla' \sigma') dv'. \quad (3.8)$$

as the part of the vector potential which contributes to the magnetic flux density. If it is assumed that the conductivity in the domain is constant, then

$$\mathbf{A} = -\frac{\mu_0}{4\pi} \sigma' \int_{s'} \frac{u'}{R} ds' \quad (3.9)$$

is the vector potential at the point \mathbf{r} .

Using vector identity 4, we see that

$$\nabla \times \frac{ds'}{R} = \frac{1}{R^3} ds' \times \mathbf{R}$$

so the magnetic flux density becomes

$$\mathbf{B} = -\frac{\mu_0}{4\pi}\sigma' \int_{s'} \frac{u'}{R^3} ds' \times \mathbf{R} \quad (3.10)$$

and hence the magnetic field may be calculated from

$$\mathbf{H} = -\frac{1}{4\pi}\sigma' \int_{s'} \frac{u'}{R^3} ds' \times \mathbf{R} \quad (3.11)$$

which is now just the integral over the surface of the domain, with u' being the electric potential on the surface.

3.2.3 Non-Constant Conductivity

The proof of eqn (3.11) relied upon there being constant conductivity within the domain, which is not guaranteed for many domains including ones filled with seawater. However this condition is unnecessary if further terms are included. Return to eqn (3.8) but assume that the conductivity of the volume is not constant. This means that to calculate the vector potential, the term

$$\int_{v'} \frac{V'}{R} (\nabla' \sigma') dv'$$

must be included.

If the domain can be divided into two subdomains, in each of which the conductivity is constant, separated by some surface s then it is easy to show that

$$\int_{v'} \frac{V'}{R} (\nabla' \sigma') dv' = \int_s \frac{V'}{R} (\sigma'_2 - \sigma'_1) ds.$$

This is another surface integral over a new surface residing within the domain. Hence the potentials on this surface need to be calculated using eqn (3.1), but once this is done the above integral may be calculated and the magnetic field found.

The details of the proof can be found in (Allan [12]), where additional results are presented.

4 The Modelling of a Ship.

Having developed and tested the procedures described above, they were then implemented on a model of an aircraft carrier with a 50,000 tonne displacement. The box of seawater occupies the space $|x| \leq 250m$, $|y| \leq 150m$, and $|z| \leq 50m$. The ship floats in the top surface parallel to the x-axis with bow at $x = 170m$ and propeller centred at $x = -82m$, $y = 0m$, and $z = 41m$. The boundary was meshed with 5132 triangles in all. On the model, the hull was coated with a protective paint which was initially intact, i.e. had high resistance. The effect of this in the real world would be that very little corrosion would occur (Zamani & Porter [2]), resulting in small amounts of current flowing in the sea about the vessel so the expected values of the magnetic field would be extremely small. Since the propeller of the

ship does not have a coating and a comparatively small area, the majority of the sea currents would be focused on this region meaning that a large peak was expected in the magnetic field about this area.

At this point it should be stated that the polarization data used at is from a idealized linear relation. Hence the current density was calculated from the surface potentials using a polarization ‘gradient’ which could be altered to account for the level of protection offered by the paint coating.

A plot of the magnitude of the calculated magnetic field at 20m below the base line of the hull is shown in figure 1. Evaluation of the field at this level is standard practice for signature engineers.

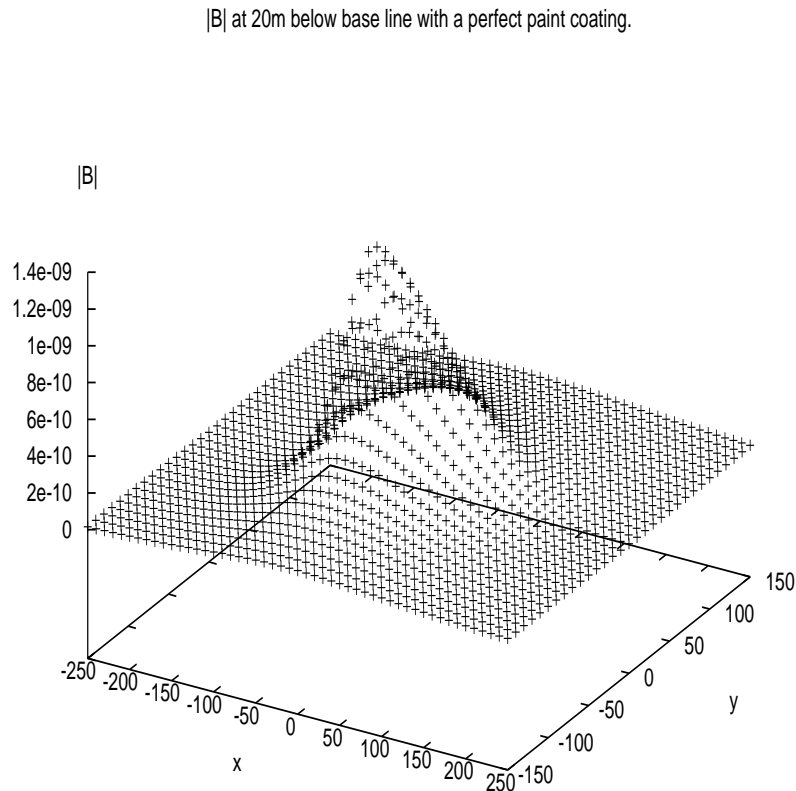


Figure 1: The magnitude of the magnetic field for the ship with a well coated hull at 20m below base line.

From the plot it can be seen that the magnitude of the field is indeed very small, and there is a sharp peak in the vicinity of the propeller. The size of the $|\mathbf{B}|$ values is not cause for great concern as it is a direct consequence of the conditions on the hull.

To show that the methods described above are capable of modelling more realistic situations a number of test calculations have been investigated. These were the cases where there are areas of paint damage on the hull, and when the ICCP anodes were activated to

try and counter the effect of the paint damage. Firstly, we considered the case when the paint on the hull in the region $133.8 \leq x \leq 153.8$ was damaged. This damage was modelled by altering the gradient of the idealized linear polarization relation used. In the first case, the damage was not overly severe, with this gradient made 1000 times larger. Physically this could occur due to either a thinning of the paint coating by a factor of one thousand, or an increase in conductivity of the paint by one thousand. The resultant effect on the magnitude of the magnetic field is shown in figure 2.

$|B|$ at 20m below base line with the paint coating slightly damaged.

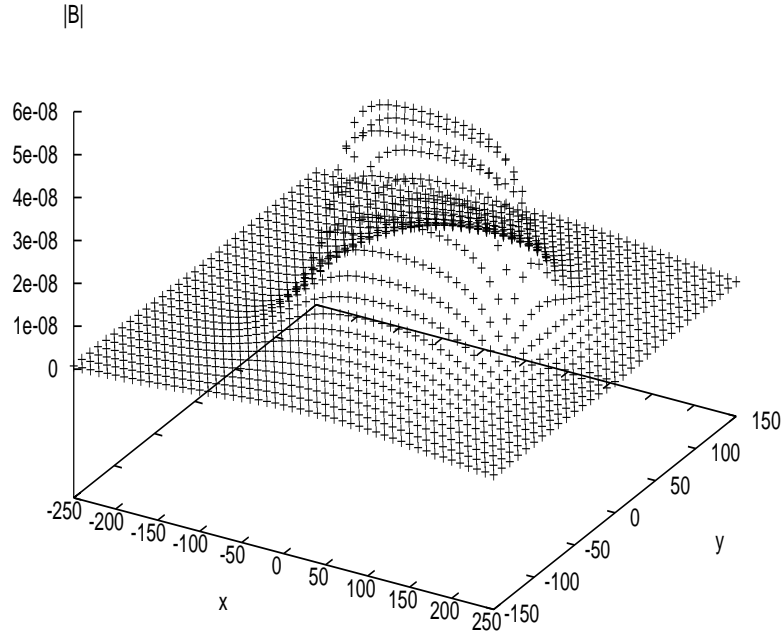


Figure 2: The magnitude of the magnetic field at 20m below base line for the ship with slightly damaged paint in the range $133.8 \leq x \leq 153.8$.

As expected, the shape of the magnitude of the magnetic field has altered. There is no longer a distinct peak around the propeller, instead there is a larger, more evenly spread field. The increase in the magnitude is a direct result of the increase in the polarization gradient. This has the effect of increasing the magnitudes of the \mathbf{q} values, which increases the current that is flowing from the hull to the propeller and hence increasing the magnetic fields. The peak around the propeller has been removed since the area of paint damage is located towards the bow of the ship, so more current is now flowing from the bow of the vessel to the propeller with the effect of spreading out the field.

The level of paint damage was then further increased for the same region of the hull, with

the polarization gradient taken to be unity for the damaged section. With reference to the original perfect paint coating, this corresponded to either a thinning of the paint by a factor of one million, or an increase in the conductivity of the paint by one million. The plot of the magnitude of the magnetic field for this case is shown in figure 3.

|B| at 20m below base line with the paint coating severely damaged.

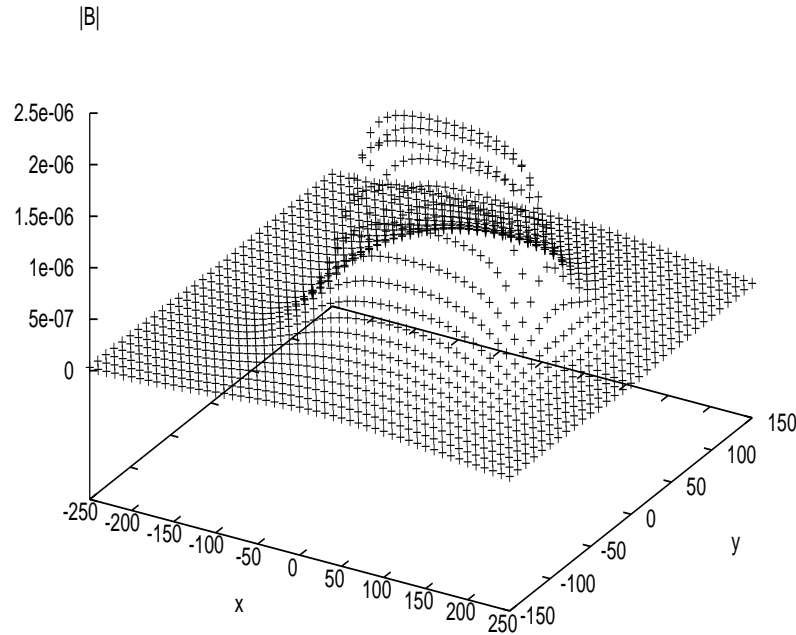


Figure 3: The magnitude of the magnetic field at 20m below base line for the ship with extremely damaged paint in the range $133.8 \leq x \leq 153.8$.

The differences between this plot and figure 1 for perfect paint are due to similar reasons as cited for the less severely damaged paint case shown in figure 2. Note that overall, the magnitude has increased on the less severely damaged case which is expected since the polarization gradient has been increased which increases the \mathbf{q} values (hence the emitted current) and therefore the magnitude of \mathbf{B} will have increased.

We now consider briefly the changes in the magnetic field due to currents to be supplied via the ICCP anodes. There are four anodes, positioned in two pairs with the members of each pair located on either side of the hull. The first pair are located towards the front of the hull, at $x = 60.67m$, while the second pair at $x = -27.00m$.

Figure 4 shows the result of the ICCP anodes being turned on, each supplying a current of 1A. By comparing figure 4 with the corresponding graph for the anodes off with the same paint damage, figure 2, it is obvious that the anodes have a large effect on the fields produced.

|B| at 20m below base line with slightly damaged paint and ICCP anodes activated.

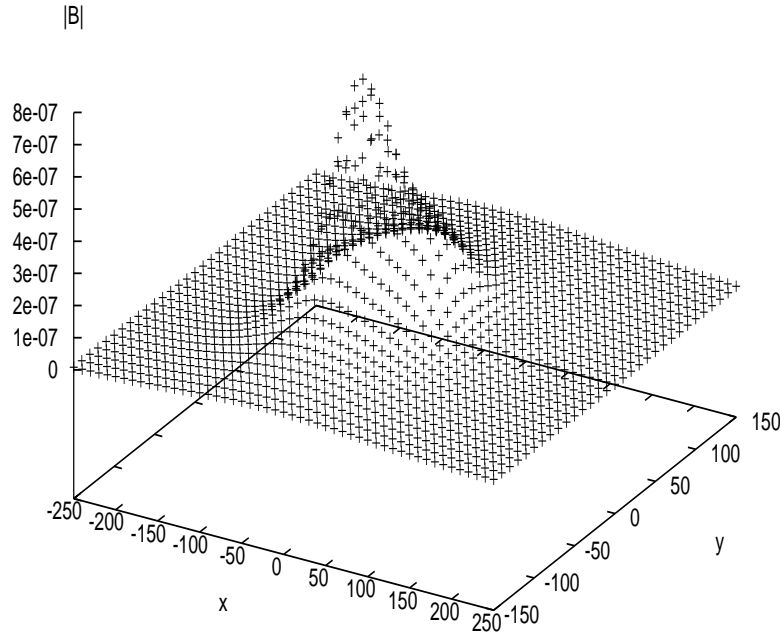


Figure 4: The magnitude of the magnetic field at 20m below base line for the ship with slightly damaged paint in the range $133.8 \leq x \leq 153.8$ and the ICCP anodes supplying 1A each.

The shape is no longer spread out, with the peak in the vicinity of the propeller reappearing and the magnitude of the field increasing compared to the plots for the previous situations. This is a direct consequence of the ICCP anodes supplying more current to the model. The reduction in spatial extent of the peak indicates that the effect of the damaged paint on \mathbf{H} has to some extent been removed by the ICCP system. However this has occurred at the expense of an overall increase in the magnitude of the field.

5 Conclusion and Discussion.

The findings presented here are broadly in agreement with other studies (Zamani & Porter [2]) of the EM signatures of marine vessels due to corrosion. Modelling this physical problem may involve a semi-infinite domain, hence the BEM is the most suitable numerical method for carrying out the analysis. The coefficient matrices of the BEM are dense hence their calculation will require tens of millions of numerical integrations to be calculated. The accuracy of the numerical integration is crucial in BEM and can be controlled but in general

to perform a reasonably accurate integration numerically takes longer than other processes such as differentiation, and summation. Hence a new method of calculating the integrals was used which focused on these issues via the formation of polynomials with a unique shape parameter as the variable (Allan [13]).

The point successive over-relaxation technique is used to solve the sets of equations in the BEM. This had the advantage for the particular problem considered here that it allows polarization restraints on \mathbf{q} to be imposed at each point as soon as our estimate of \mathbf{u} changes.

To compute the magnetic field \mathbf{H} resulting from corrosion currents, a method was derived which allows \mathbf{H} to be computed directly from the electric potentials on the boundaries. This has the great advantage that it does not require intermediate values of electric potential, electric field and current to be calculated throughout the volume with a subsequent volume integration of the Biot-Savarts Law to find \mathbf{H} , but computes \mathbf{H} directly from the output from the BEM. This method has been validated using classical problems (Allan [12]).

Preliminary calculations for various conditions on the hull show that these methods are perfectly capable of evaluating the electromagnetic fields. By comparing the magnetic fields produced for the cases of a perfect paint coating, a slightly damaged paint coating, a severely damaged paint coating, and a slightly damaged paint coating with ICCP anodes turned on, it is clear that these methods give plausible results. Further research is necessary in these areas with one of the key requirements being the inclusion of more realistic polarization data. Until this has been done, no meaningful comparison can be drawn between the results provided by these methods and experiment.

More details of the methods described in this paper and additional results and analysis may be found in a thesis by one of the authors (Allan [12]).

6 Acknowledgements

One of us, P. Allan, is grateful for the financial support from PPARC and BAE Systems.

References

- [1] Jeffery, I. & Brooking, B., *A Survey of New Electromagnetic Stealth Technologies*, www1.davis-eng.com/docs/New_Electromagnetic_Stealth.pdf
- [2] Zamani, N.G., & Porter, J.F., Boundary Element Simulation of the Cathodic Protection System in the Destroyer Class 280. *Boundary Element Techniques: Applications in Fluid Flow and Computation Aspects*, eds. C.A. Brebbia & W.S. Venturini, Computational Mechanics Publications, pp. 123-138, 1987.
- [3] Wang, Y., Brennan, D.P., Porter, J.F., & Karisallen, K.J., Evaluation of a Shipboard ICCP System using Boundary Element Code. *2nd International Warship Cathodic Protection Symposium*, Cranfield University, 2003.

- [4] Brebbia, C.A., *The Boundary Element Method for Engineers*, Pentach Press, 1978.
- [5] Symm, G.T., An Introduction to the Application of Boundary Element Methods in Electrostatics. *BETECH 86 - Proceedings of the 2nd Boundary Element Technology Conference*, eds. Connor, J.J. & Brebbia, C.A., Computational Mechanics Publications, pp. 63-75, 1986.
- [6] Defouny, M., The Boundary Element Method Applied to Electric Field Computation: Generation, Computation and Results with Examples in the High Voltage Field. *BETECH 86 - Proceedings of the 2nd Boundary Element Technology Conference*, eds. Connor, J.J. & Brebbia, C.A., Computational Mechanics Publications, pp 75-84, 1986.
- [7] Press, W.H., Flannery, B.P., Teubolsky, S.A., & Vetterling, W.T., *Numerical Recipes in C: The Art of Scientific Computing*, Cambridge University Press, 1988.
- [8] Jansson, P.A., *Deconvolution of Images and Spectra (Second Edition)*, Academic Press, 1997.
- [9] Bencham, S.P., & Lord, J.A., *EMMA_F:FM3D. Theory and Initial Results from a Multi-Level Fast Multi-pole Code*, BAe Systems Advanced Technology Centre (Sowerby) (Confidential in Commerce)
- [10] Adey, R.A., Brebbia, C.A., & Niku, S.M., BEASY-CP - A System for Analysis of Galvanic Corrosion and Cathodic Protection using Boundary Elements. *BETECH 86 - Proceedings of the 2nd Boundary Element Technology Conference*, eds. Connor, J.J. & Brebbia, C.A., Computational Mechanics Publications, pp. 85-108, 1986.
- [11] Kermorgant, H., Modelling and Characterization of the Underwater Electromagnetic Field Radiated by an UUV in the Static Domain. *MARELEC '99 - 2nd International Conference on Marine Electromagnetics*, pp. 459-469, 1999.
- [12] Allan, P.J., *Ph. D Thesis, A Study of the Electromagnetic Signatures of Marine Vessels using the Boundary Element Method*, University of Glasgow, 2004.
- [13] Allan, P.J. and Watt, A., A Study of Corrosion Related Magnetic Signatures of Marine Vessels using a BEM. *Proc. of BEM 26*, WIT 2004.
- [14] Young, H. D. and Freedman, N. A., *University Physics (Extended version with modern physics) 9th Edition*, pp.913-914, Addison-Wesley Publishing Company, Inc., 1996.
- [15] Boas M L. *Mathematical Methods in the Physical Sciences*, John Wiley and Sons, 1983.

- [16] Lorrain, P., Corson, D., & Lorrain, F., *Electromagnetic Fields and Waves*, W.H. Freeman & Company, 1996.